

Serum total periostin is an independent marker of overall survival in bone metastases of lung adenocarcinoma

E Massy, J. C. Rousseau, M. Gueye, E. Bonnelye, M. Brevet, L. Chambard, M. Duruisseaux, O. Borel, C. Roger, R. Guelminger, et al.

▶ **To cite this version:**

E Massy, J. C. Rousseau, M. Gueye, E. Bonnelye, M. Brevet, et al.. Serum total periostin is an independent marker of overall survival in bone metastases of lung adenocarcinoma. Journal of Bone Oncology, 2021, 29, pp.100364. 10.1016/j.jbo.2021.100364 . hal-03263846

HAL Id: hal-03263846
https://cnrs.hal.science/hal-03263846

Submitted on 17 Jun 2021

HAL is a multi-disciplinary open access archive for the deposit and dissemination of scientific research documents, whether they are published or not. The documents may come from teaching and research institutions in France or abroad, or from public or private research centers.

L'archive ouverte pluridisciplinaire **HAL**, est destinée au dépôt et à la diffusion de documents scientifiques de niveau recherche, publiés ou non, émanant des établissements d'enseignement et de recherche français ou étrangers, des laboratoires publics ou privés.

Manuscript File Click here to view linked References

Serum total periostin is an independent marker of overall survival in bone metastases of adenocarcinoma lung cancers

E Massy[1,2,3*] ; JC. Rousseau [1*]; M. Gueye [3] ; E. Bonnelye [1,4] ; M. Brevet [2,5] ; L. Chambard [3] ; M. Duruisseaux [2,6] ; O. Borel [1] ; C. Roger [1,7] ; R. Guelminger [6] ; JB. Pialat [8] ; E. Gineyts [1] ; L. Bouazza [1] ; M. Millet [1] ; JM. Maury [9] ; P. Clézardin [1,2] ; N. Girard[10] ; Cyrille B. Confavreux[1,2,3]

[1]: INSERM UMR 1033-LYOS, Lyon, France
[2]: Université de Lyon
[3]: Centre Expert des Métastases Osseuses (CEMOS) - Service de Rhumatologie, Centre Hospitalier Lyon-Sud, Hospices Civils de Lyon, Pierre-Bénite, France
[4]: CNRS ERL 6001/ INSERM U1232-Institut de Cancérologie de l'Ouest-Université de Nantes
[5]: Anatomie pathologique, Hospices Civils de Lyon, Lyon
[6]: Service d'Oncologie Thoracique, Hôpital Louis Pradel, Hospices Civils de Lyon, Lyon
[7]: Biochimie centre hospitalier Lyon sud, INSERM UMR 1033 - Hospices Civils de Lyon, Lyon, France
[8]: Service de Radiologie, Centre Hospitalier Lyon-Sud, Hospices Civils de Lyon, Pierre-Bénite, France
[9]: Chirurgie thoracique, Hôpital Louis Pradel, Hospices Civils de Lyon, Lyon
[10]: Pneumologie, Institut du thorax Curie-Montsouris, Paris

* These authors have contributed equally to this work.

Correspondance
Pr Cyrille B. CONFAVREUX, MD PhD
ORCID: 0000-0002-9318-6785
Service de Rhumatologie Hôpital Lyon Sud
165 chemin du Grand Revoyet
69310 Pierre Bénite, France
E-mail: cyrille.confavreux@chu-lyon.fr
Clinical Trial registration number: NCT 028 102 62
The study was accepted by the local ethics committee (Institutional Review Board N° 11263 – CPP Sud-Est II)

Word count: 3193
Tables: 3 Figures: 3 Supplementals: 3

Conflict of interest statement:
The authors declare that there is no conflict of interest regarding the publication of this article

FUNDING
Young Researcher Grant from the Hospices Civils de Lyon (CC), Grant (CC and NG) from the GIRCI AURA (Groupement Inter-Régionaux pour la Recherche Clinique en Région Auvergne Rhone-Alpes), DREAMER-Novartis rheumatology research grant (CC), Centre National de la Recherche Scientifique CNRS (EB), Institut National de la Santé et de la Recherche Médicale INSERM (CC, JCR).

ABSTRACT

250 words

More than 35% of adenocarcinoma lung cancers present with bone metastases at diagnosis and have a poor survival. Periostin, a carboxylated matrix protein, is involved in lung cancer cell dissemination through epithelial-mesenchymal transition, in bone response to mechanical stress and in bone formation regulation. Thus, periostin is a candidate biomarker for bone metastasis severity and lung cancer patient survival.

Serum periostin was assessed at diagnosis in a prospective cohort of 133 patients with adenocarcinoma lung cancer of all stages. Patients were divided into localized and bone metastatic groups. Both groups were matched to healthy controls. Survival analysis and Cox proportional hazards models were conducted in the total population and in bone metastatic group.

The median serum periostin level was higher in bone metastatic (n=67; median: 1752pmol/L) than in the localized group (n=66; 861pmol/L; p<0.0001). Patients with high periostin (>median) had a poorer overall survival in the whole population (33.3 weeks vs. NR; p<0.0001) and the bone metastatic group (24.4 vs. 66.1 weeks; p<0.001). In multivariate analysis, patients with high periostin had increased risk of death (HR=2.09, 95%CI [1.06-4.13]; p=0.03). This was also found in the bone metastatic group (HR=3.62, 95%CI [1.74-7.52]; p=0.0005). Immunohistochemistry (IHC) on bone metastasis biopsies found some periostin expression in bone matrix and in cancer cells (nuclear and cytoplasmic).

Serum periostin was an independent survival biomarker in all-stage and in bone metastatic adenocarcinoma lung cancer patients. IHC data suggest that periostin might be induced in cancer cells in bone metastatic niche in addition to bone microenvironment expression.

Keywords: bone metastasis; periostin; lung cancer; serum biomarker; survival

INTRODUCTION

Lung cancers are leading cause of cancer mortality in France (1). Non-small cell lung cancer (NSCLC) accounts for up to 85% of lung cancer (2) and 35 to 50% of lung cancers have bone metastasis at the time of cancer diagnosis or will develop bone metastasis (3). When first diagnosed, more than 30% of lung cancer patients are at an advanced stage, including bone metastases; those with advanced lung cancers have a poor survival outcome (2) and this is particularly the case for patients with bone metastasis (4).

Locally, bone metastasis is characterized by the establishment of a metastatic niche (5). A worldwide effort is ongoing to understand, predict, and treat bone metastasis at the earliest stages of metastatic niche (5). Dissemination of tumor cells occurs early and seems to be a frequent event (6), for which a key step is epithelial-mesenchymal transition (EMT) of carcinoma cells that confers increased invasion and metastasis properties to NSCLC cells (7).

Periostin is a 19kD carboxylated matrix protein found in various extracellular matrices, including the lung and bone (8). Periostin is made of a NH2-terminal signal peptide sequence, an internal homologous repeat region, cysteine-rich domains, and a hydrophilic COOH-terminal domain. In bone physiology, periostin is involved in the response to mechanical stress, and bone formation regulation through the control of sclerostin expression in the periosteum (9). Periostin has been also implicated in energy metabolism, in cell function regulation, and cell-matrix interactions (10). In addition, periostin is thought to promote EMT by targeting the crosstalk between the epidermal growth factor (EGFR) and the integrins at the plasma membrane, with consecutive activation of the Akt/PKB (protein kinase B) and the FAK (focal adhesion kinase) pathway (11).

Periostin cancer expression has been associated with poor survival outcomes in a heterogenous group of tumors (12). In NSCLC, Zhang et al. reported that periostin serum level was higher in advanced stage III/IV than in various benign lung diseases and periostin was associated with the presence of bone metastases (13). They have also found that periostin was associated with the time to first progression, but the origin of periostin is not fully understood. We therefore first investigated whether periostin serum level at diagnosis, before any oncological treatment, was associated with overall survival in patients with adenocarcinoma lung cancers of all stages and specifically in those with bone metastases. Then, since *KRAS* mutation is the most frequently found mutation in human adenocarcinoma lung cancer bone metastases, and is responsible for high affinity and agressivity towards the bone (14), we focused on bone metastasis biopsies with *KRAS* mutation to describe periostin expression using immunohistochemistry (IHC). Finally, we compared the IHC results to our *in vivo* model of bone metastasis with A549 *KRAS*-mutated cells.

MATERIALS AND METHODS

Patients and controls.

The POUMOS project is a single-center non-interventional prospective cohort of NSCLC developed within the Hospices Civils de Lyon, Lyon, France. The project started in 2010 and has been approved by the French ministry of research and the regional ethics committee (*Comité de protection des personnes Lyon Sud-Est IV – protocol number 11.460*), and has been registered on ClinicalTrial.Gov; number: 028 102 62); all patients provided a written informed consent. The present study has two groups: patients with non-metastatic adenocarcinoma lung cancer requiring lung surgery (these patients could be stage I, II or III) and patients presenting a first bone metastasis from adenocarcinoma lung cancer confirmed by bone metastasis biopsy (stage IV). Patients should not have previously received any systemic treatment (chemotherapy, targeted therapy, or immune checkpoint inhibitor) to be included. Data regarding cancer and patient characteristics were collected. Advanced lung cancer inflammation index (ALI) was computed as follows: body mass index (Kg/m²) x serum albumin (g/L) / neutrophil-lymphocyte ratio (NLR). Patients were prospectively followed until death. Patients underwent blood sampling before any oncological treatment including systemic treatment, radiotherapy, or surgery. Standard laboratory tests were performed according to routine procedures. Sera were stored at -80°C until the periostin assay was performed. For the present study, patients from each group of the cohort were paired according to age (± 1 year) and sex to healthy controls available in our rheumatology cohorts in Lyon composed of healthy adults. These cohorts were designed to achieve bone density standards in healthy subjects (15, 16); one control could be matched to one patient of each group. None of the control patients had cancer.

Periostin assay.

Serum periostin was assessed using the ELISA kit (Biomedica®, Vienna, Austria) (17). Briefly, plates were coated with 150 µL of the mouse monoclonal anti-human periostin coating antibody, sealed and incubated for one hour at room temperature (18-26°C). After aspiration of the coating solution, wells were blocked with 300 µL per well of blocking solution overnight at 4°C. Thereafter, each well was aspirated and dried for three hours. Human serum samples were diluted 1/50 with phosphate buffered assay (PBS), and 150 µL of this solution were added to the dried wells and incubated for two hours at room temperature. Plates were then washed five times with washing buffer before adding 150 µL of the biotinylated goat polyclonal anti-human periostin antibody and incubated for two hours at room temperature. Plates were washed five times as described before. In order to detect bound biotinylated detection antibody, 150 µL of the conjugate solution, consisting of horseradish peroxidase (HRP) -

labeled streptavidin, was added to each well. The mixture was incubated for one hour at room temperature to allow the formation of the biotin-streptavidin complex. After incubation, wells were washed five times, and substrate solution was added. The final incubation step was performed in the dark, and the reaction was stopped after 30 minutes with stop solution. The absorbance at 450 nm was measured using a microplate reader.

Periostin immunohistochemistry on bone metastases sections

Four-micron paraffin sections of bone metastasis, from *KRAS* and non-*KRAS* mutated adenocarcinoma lung cancers, were incubated overnight with anti-mouse/human periostin (1/1000; Biomedica®, Vienna, Austria) or with anti-mouse/human periostin (1/500; USCN®, Wuhan China) followed by incubation with HRP-conjugated anti-rabbit antibodies (1/300; Dako Agilent®, Santa Clara, CA USA) for 1 hour and staining with 3,3'-diaminobenzidine (Dako Agilent®, Santa Clara, CA USA) and Mayer's hematoxylin (Merck-Sigma-Aldrich®, Darmstadt, Germany). For the *in vivo* model, anti-mouse/human periostin was used at a dilution of 1/200; the secondary antibody was anti-goat (1/300; Jackson®, Bar Harbor, MA USA).

Cell line

The human A549 *KRAS*-mutated cancer cell line was bought from the ATCC® Manassas, VI USA (ATCC CCL-185™), and cultured in F-12K medium (Life-Technologies® Carlsbad, CA USA), supplemented with 10% fetal bovine serum (Perbio®, Waltham, MA USA) and 1% penicillin/streptomycin (Invitrogen®, Carlsbad, CA USA) at 37°C in a 5% CO_2 atmosphere. Cultured cells were tested for mycoplasma regularly.

In vivo bone metastases mouse model

Four-week-old BALB/c female nude mice (Janvier Labs®, Le Genest St Ile France) (n=5) were purchased and housed for 2 weeks in a specific-pathogen-free facility (ALECS platform, Faculté de Médecine Laennec, Lyon, France). After two weeks of housing, mice were anesthetized with intraperitoneal injection of 20µL/g of ketamine 130mg/kg and xylazine 8.8mg/kg diluted in physiological serum and injected intracardiac with 100µL of A549 tumor cell solution ($1*10^6$ cells/mL of sterile PBS). The development of bone metastases was assessed weekly on plain radiographs (X-rays set-up: 18kV-35s; Faxitron®, Tucson, AZ USA). At day 30, mice were sacrificed and hind limbs were then collected, fixed with paraformaldehyde 4% for 24 hours, rinsed with PBS and then processed according to the routine histology procedure. Four-micron paraffin sections were obtained and stained with hematoxylin and eosin. Mice protocol followed was approved by the animal ethics committee of Lyon I university (IRB approval number: BH2012-05).

Statistical analysis

The Spearman's correlation coefficients were used to assess the correlations between periostin and clinical or laboratory parameters. Boxplots were used to visualize the distribution of periostin in the metastatic, localized, and control group. Student's t and Wilcoxon's tests were used to compare groups. Overall survival (OS) between patients with high periostin serum level (greater than the median) vs. low periostin serum level was estimated and compared using the Kaplan-Meier method and the Log-rank test in the total population and in the bone metastatic group. Parameters associated with survival were analyzed and a multivariate Cox proportional hazards model was used to determine the influence of periostin and covariates on overall survival. All analyses were conducted using R statistical software (Version 3.6.0). A p-value below 0.05 was considered statistically significant in all analysis.

RESULTS

Baseline characteristics

A total of 133 patients with an adenocarcinoma lung cancer were included between February 2010 and October 2018. There were 84 (63%) men, and the mean ± SD age was 63.5 ± 10.9 years (Table 1). Among these, 67 patients were included in the localized group and 66 in the metastatic group. Patients of each group were paired 1:1 to healthy controls (63 men and 41 women) for periostin serum assay.

There was no significant difference in mean ± SD age at inclusion between metastatic (65.1 ± 11.6 years) and localized groups (61.9 ± 10.0 years; p=0.27). All patients in the metastatic group had bone metastases among which 19 patients (29% of metastatic group) were bone metastatic only without any soft tissue involvement at the inclusion and 47 patients (71% of metastatic group) present with both soft tissue and bone metastases. Patients of the metastatic group had a significantly lower mean ± SD serum albumin level (33.9 ± 5.6 g/L vs. 37.8 ± 4.1 g/L; p=0001); a significantly higher inflammatory status, as reflected by mean ± SD C-reactive protein (CRP; 61.8 ± 67.6 mg/L vs. 15.6 ± 43 mg/L; p=0.0006) or NLR (5.1 ± 4.8 vs. 3.4 ± 5.3; p=0.0005); and a significantly lower mean ± SD ALI index (189.2 ± 161.3 vs. 365.8 ± 305.4; p=0.0008). Regarding bone parameters, no significant difference was observed for bone phosphatase alkaline but mean ± SD calcemia (2.29 ± 0.2 mmol/L vs. 2.18 ± 0.8 mmol/L; p=0.02) and mean ± SD serum carboxy-terminal collagen crosslinks (CTX; 700 ± 375.9 pg/mL vs. 488.3 ± 285.2 pg/mL; p=0.0004) were significantly higher in the metastatic arm.

Total serum periostin assay

In the total population, the mean ± SD serum periostin level was 1307 ± 656 pmol/L and the median level was 1092 pmol/L. Periostin was not correlated with age but with inflammation parameters : CRP (r=0.50; p=0.0005), albuminemia (r=-0.33; p=0.001), and NLR (r=0.36; p=0.003). Regarding bone parameters, serum periostin was correlated with serum CTX (r=0.26; p=0.002) but not with calcium serum level or bone alkaline phosphatase (data not shown).

The median serum periostin level in the localized group was slightly different than in matched healthy controls (861 vs. 1004 pmol/L; p=0.01) whereas in the bone metastatic group it was 70% higher than its controls (1752 vs. 1033 pmol/L; p<0.0001) and twice that found in the localized group (p<0.0001; Supplemental figure 1).

Overall survival

Median [95% CI] follow-up duration was 57.9 [1.3-350.0] weeks. Median OS was 84.3 [57.7-110.8] weeks (1.6 years) in the total population. Median OS was 32.9 [25.0-40.7] weeks in the metastatic group and was not reached (NR) in localized group (Log-rank p<0.0006). A high (>median) serum periostin level at inclusion was associated with a shorter survival (median: 33.3 weeks vs. NR; p<0.0001, Figure 1A) and a higher risk of death (HR=5.20, 95% CI [3.03 to 8.90]; p<0.0001). Other parameters significantly associated with an increased risk of death were age, metastatic status, high CRP, low albumin serum level, high calcemia, high NLR and high ALI, (Table 2). In the multivariate Cox proportional hazards model, including periostin, metastatic status, age, CRP, ALI, CTX and calcemia, only metastatic status (HR=2.09, 95% CI [1.06-4.13]; p=0.03) and high periostin (HR=2.80, 95% CI [1.59-4.95]; p=0.0003) were significantly associated with an increased risk of death (Table 2).

Overall survival in the bone metastatic arm

In the bone metastatic arm, high periostin and low albuminemia were associated with an increased risk of death (Figure 1B and Table 3). In the Cox model including periostin, age, CRP, ALI, CTX and calcium serum level, high periostin remained associated with an increased risk of death (HR=3.62 [1.74-7.52]; p=0.0005, Table 3).

Periostin IHC on patient bone metastasis

Paraffin sections of bone metastasis were available from 10 patients; including n=5 *KRAS* mutated, and n=5 *KRAS*-non mutated adenocarcinoma lung cancers. As expected, periostin was present in tumor-associated stroma. Interestingly, and there was also an expression by some tumor cells; this expression was heterogenous, mostly cytoplasmic and sometimes nuclear (Figure 2, and supplemental Figures 2 and 3).

Exploratory in vivo experiments of NSCLC bone metastasis

Using osteolytic bone metastasis generated in *nude* mice (Figure 3a and b), IHC analysis found an intranuclear tumor expression of periostin in some bone metastases (Figure 3 d-f); no expression was observed on the A549 cell line (Figure 3c) *in vitro* cultures suggesting a tumor induction of periostin in the bone microenvironment.

DISCUSSION

In the present study, we found that high serum periostin level was independently associated with an increased mortality in all adenocarcinoma lung cancers and in the bone metastatic arm. We observed by IHC of bone metastases that periostin was expressed in the bone microenvironment but also in some cancer cells with nuclear and cytoplasmic expression. To our knowledge, there was no previous report on adenocarcinoma lung cancers looking for both serum periostin levels and immunochemistry in bone metastases. In addition, the exploratory *in vivo* experiment of bone metastasis with *KRAS* A549 cell line, suggested that periostin expression by cancer cells, might be induced by bone microenvironment.

Serum periostin has been previously reported as a poor prognosis marker in different types of cancers (12), including NSCLC, Xu et al. and Zhang et al. showed that serum periostin levels were increased in NSCLC patients compared with benign lung diseases and controls (13,18). Nevertheless, their controls were not paired to the cancer patients. High serum periostin level was associated with shorter time to first progression and an advanced stage of the disease (13, 18). Herein, we go further with paired controls, overall survival and focus on bone metastasis of adenocarcinoma lung cancer. The multivariate analysis included inflammation prognostic markers such as ALI index and CRP, and CTX bone turnover marker. Thus prognosis value of serum periostin at the time of diagnosis, before any treatment, irrespective of the stage, was clearly underlined here.

Nevertheless, the origin of periostin in serum was not obvious. Firstly, in the IHC we clearly observed in some patients a strong bone stroma reaction independently of the expression of cancer cells. From a physiological point of view, this is consistent with the described role of periostin in bone anabolism by Bonnet *et al.*; in response to mechanical stress, osteoblasts and osteocytes overexpress periostin that blocks sclerostin and thus enhances all aspects of bone anabolism such as mineralization and osteoblast proliferation (19). This reaction, by increasing bone mass and cortical bone, may contribute to strengthen the bone to face the osteolysis induced by the metastasis. Furthermore, in bone metastatic microenvironment, periostin could be secreted by other cells in the stroma such as cancer-associated fibroblasts, myofibroblasts, or bone marrow-derived mesenchymal stem cells (8). In a feedback loop, this bone expression of periostin may have an impact on lung cancer cell proliferation. Indeed, it has been reported that periostin promotes the survival of A549 cells *via* activation of the AKT pathway (20). Periostin could also promote EMT in lung cancer by activating the p38/ERK pathway and repressing the expression of microRNA-381 that targets both Snail and Twist (21). Thus, the cancer stimulation might be local at the bone metastatic site but also in a more systemic manner including the primary site of the tumor.

Secondly, we also observed by IHC a cancer cell intranuclear and cytoplasmic expression of periostin. Further studies are required to understand the physiological role of these different locations in tumor cells. This observation was made both in human bone metastasis biopsies and in the *in vivo* A549 bone metastatic mouse model. This local production of periostin by bone metastasis may promote osteolysis since Che *et al.* previously published that the silencing of periostin in lung cancer cell lines reduces osteoclastogenesis and osteoclast activity through αvβ3 integrin signaling (22). They also observed a reduction of osteolytic bone metastases in vivo.

Beyond the findings in bone metastases, we observed that serum periostin was a biomarker of poor survival in the adenocarcinoma lung cancer population. This poor prognosis has also been reported in other types of cancer (21,22,23,24,25) suggesting that it was not restricted to lung cancer. Periostin oncologic potency corresponds to its stimulatory effect on cancer cells as previously discussed but also to its expression by cancer cells themselves. For example, periostin is overexpressed in localized breast cancer. This overexpression was not dependent on disseminated tumor cells status (28). In lung cancer, periostin was significantly increased in cisplatin-resistant A549 cells compared with parental cells, and overexpressing periostin rendered A549 cells more resistant to cisplatin-induced apoptosis *via* activation of STAT3 and upregulation of Survivin (29). In another model of lung cancer using SBC-5 cells, Che *et al.* silenced periostin that decreased agressivity of the cells (migration, proliferation and secretion of metastasis associated factors) (22). Taken together, these studies showed an important role of periostin in tumor cell proliferation, survival, angiogenesis, invasion, metastasis and chemoresistance.

Interestingly, the *in vivo* exploratory model, which is a good way to generate hypothesis, found that there might be an induction of periostin expression by A549 cancer cells in the bone microenvironment. This result was supported by a previous report showing that periostin expression could be induced by TGF-α and βFGF under the stress of chemical-mimic hypoxia in A549 NSCLC cells(20). We acknowledge, however, that for human IHC, we only had bone metastatic tissue and these were not paired with primitive tumor preventing formal conclusion as to the induction of expression by bone metastatic niche cancer cells.

At this stage all three sources (the cancer cells, the bone, and the bone microenvironment) might release periostin to the blood. The ELISA kit used for this study recognizes all types of periostin, but, considering the different sources of periostin previously discussed, there might be some isotypes more specific of bone, cancer cells, or soft tissue. This is supported by the study reported by Morra *et al.* that described nine different isoforms of periostin and identified five of them in lung biopsies of NSCLC. In lung biopsies, both tumor stroma and epithelium expressed periostin (30). In bone, Bonnet *et al.* also reported that specific fragment (K-Postn) are released after cathepsin K digestion (31). This question of

specific periostin fragments is currently under investigation. The current challenge is to develop periostin ELISA kits able to specifically detect bone metastatic released fragments.

In conclusion, serum total periostin level was a prognostic biomarker of poor overall survival in all-stage adenocarcinoma lung cancers and in the bone metastatic group.

Periostin expression in bone metastases was heterogenous from one to another patient but in bone metastatic niche, we observed periostin expression in stroma and in lung cancer cells (intranuclear and cytoplasmic expression). Moreover, *in vivo* data suggest that periostin might be induced by bone metastatic lung cancer cells. Taken together both the literature and that reported herein, the data support that periostin expression, irrespective of the source in the bone metastatic niche, contributes to enhance cancer agressivity.

FUNDING

Young Researcher Grant from the Hospices Civils de Lyon (CC), Grant (CC and NG) from the GIRCI AURA (Groupement Inter-Régionaux pour la Recherche Clinique en Région Auvergne Rhone-Alpes), DREAMER-Novartis rheumatology research grant (CC), Centre National de la Recherche Scientifique CNRS (EB), Institut National de la Santé et de la Recherche Médicale INSERM (CC, JCR).

ACKNOWLEDGMENTS

The authors thank the Biological Resource Centre (BRC) of Hospices Civils de Lyon NeuroBioTec (CRB-HCL: BB-0033-00046), Pr Francoise Thivolet, MD PhD and Gabriela Berg (Biomedica Inc®) for their support and advice. Philip Robinson for his careful advice during editing.

REFERENCES

1. Ferlay J, Colombet M, Soerjomataram I, Dyba T, Randi G, Bettio M, et al. Cancer incidence and mortality patterns in Europe: Estimates for 40 countries and 25 major cancers in 2018. Eur J Cancer Oxf Engl 1990. 2018;103:356‑87.

2. Duma N, Santana-Davila R, Molina JR. Non-Small Cell Lung Cancer: Epidemiology, Screening, Diagnosis, and Treatment. Mayo Clin Proc. 2019;94(8):1623‑40.

3. Huang J-F, Shen J, Li X, Rengan R, Silvestris N, Wang M, et al. Incidence of patients with bone metastases at diagnosis of solid tumors in adults: a large population-based study. Ann Transl Med. avr 2020;8(7):482.

4. Chambard L, Girard N, Ollier E, Rousseau J-C, Duboeuf F, Carlier M-C, et al. Bone, muscle, and metabolic parameters predict survival in patients with synchronous bone metastases from lung cancers. Bone. 2018;108:202‑9.

5. Malanchi I, Santamaria-Martínez A, Susanto E, Peng H, Lehr H-A, Delaloye J-F, et al. Interactions between cancer stem cells and their niche govern metastatic colonization. Nature. 7 déc 2011;481(7379):85‑9.

6. Hüsemann Y, Geigl JB, Schubert F, Musiani P, Meyer M, Burghart E, et al. Systemic spread is an early step in breast cancer. Cancer Cell. janv 2008;13(1):58‑68.

7. Soltermann A, Tischler V, Arbogast S, Braun J, Probst-Hensch N, Weder W, et al. Prognostic significance of epithelial-mesenchymal and mesenchymal-epithelial transition protein expression in non-small cell lung cancer. Clin Cancer Res Off J Am Assoc Cancer Res. 15 nov 2008;14(22):7430‑7.

8. Kudo A. Periostin. Springer. 2019. (Advance in Experimental Medicine and Biology; vol. 1132).

9. Bonnet N, Standley KN, Bianchi EN, Stadelmann V, Foti M, Conway SJ, et al. The matricellular protein periostin is required for sost inhibition and the anabolic response to mechanical loading and physical activity. J Biol Chem. 18 déc 2009;284(51):35939‑50.

10. Bonnet N, Garnero P, Ferrari S. Periostin action in bone. Mol Cell Endocrinol. 05 2016;432:75‑82.

11. Yan W, Shao R. Transduction of a mesenchyme-specific gene periostin into 293T cells induces cell invasive activity through epithelial-mesenchymal transformation. J Biol Chem. 14 juill 2006;281(28):19700‑8.

12. Yang T, Deng Z, Pan Z, Qian Y, Yao W, Wang J. Prognostic value of periostin in multiple solid cancers: A systematic review with meta-analysis. J Cell Physiol. mars 2020;235(3):2800‑8.

13. Zhang Y, Yuan D, Yao Y, Sun W, Shi Y, Su X. Predictive and prognostic value of serum periostin in advanced non-small cell lung cancer patients receiving chemotherapy. Tumour Biol J Int Soc Oncodevelopmental Biol Med. mai 2017;39(5):1010428317698367.

14. Confavreux CB, Girard N, Pialat J-B, Bringuier P-P, Devouassoux-Shisheboran M, Rousseau J-C, et al. Mutational profiling of bone metastases from lung

adenocarcinoma: results of a prospective study (POUMOS-TEC). BoneKEy Rep. 2014;3:580.

15. Chaitou A, Boutroy S, Vilayphiou N, Munoz F, Delmas PD, Chapurlat R, et al. Association between bone turnover rate and bone microarchitecture in men: The STRAMBO study: BONE TURNOVER RATE AND BONE MICROARCHITECTURE IN MEN. J Bone Miner Res. nov 2010;25(11):2313‑23.

16. Sornay-Rendu E, Karras-Guillibert C, Munoz F, Claustrat B, Chapurlat RD. Age determines longitudinal changes in body composition better than menopausal and bone status: The OFELY study. J Bone Miner Res. mars 2012;27(3):628‑36.

17. Gadermaier E, Tesarz M, Suciu AA-M, Wallwitz J, Berg G, Himmler G. Characterization of a sandwich ELISA for the quantification of all human periostin isoforms. J Clin Lab Anal. févr 2018;32(2):e22252.

18. Xu C-H, Wang W, Lin Y, Qian L-H, Zhang X-W, Wang Q-B, et al. Diagnostic and prognostic value of serum periostin in patients with non-small cell lung cancer. Oncotarget. 21 mars 2017;8(12):18746‑53.

19. Bonnet N, Conway SJ, Ferrari SL. Regulation of beta catenin signaling and parathyroid hormone anabolic effects in bone by the matricellular protein periostin. Proc Natl Acad Sci. 11 sept 2012;109(37):15048‑53.

20. Ouyang G, Liu M, Ruan K, Song G, Mao Y, Bao S. Upregulated expression of periostin by hypoxia in non-small-cell lung cancer cells promotes cell survival via the Akt/PKB pathway. Cancer Lett. 28 août 2009;281(2):213‑9.

21. Hu W-W, Chen P-C, Chen J-M, Wu Y-M, Liu P-Y, Lu C-H, et al. Periostin promotes epithelial-mesenchymal transition via the MAPK/miR-381 axis in lung cancer. Oncotarget. 22 sept 2017;8(37):62248‑60.

22. Che J, Shen W-Z, Deng Y, Dai Y-H, Liao Y-D, Yuan X-L, et al. Effects of lentivirus-mediated silencing of Periostin on tumor microenvironment and bone metastasis via the integrin-signaling pathway in lung cancer. Life Sci. août 2017;182:10‑21.

23. Liu G-X. Role of periostin and its antagonist PNDA-3 in gastric cancer metastasis. World J Gastroenterol. 2015;21(9):2605.

24. Hong L-Z, Wei X-W, Chen J-F, Shi Y. Overexpression of periostin predicts poor prognosis in non-small cell lung cancer. Oncol Lett. déc 2013;6(6):1595‑603.

25. Kikuchi Y, Kashima TG, Nishiyama T, Shimazu K, Morishita Y, Shimazaki M, et al. Periostin Is Expressed in Pericryptal Fibroblasts and Cancer-associated Fibroblasts in the Colon. J Histochem Cytochem. août 2008;56(8):753‑64.

26. Ratajczak-Wielgomas K, Grzegrzolka J, Piotrowska A, Gomulkiewicz A, Witkiewicz W, Dziegiel P. Periostin expression in cancer-associated fibroblasts of invasive ductal breast carcinoma. Oncol Rep. nov 2016;36(5):2745‑54.

27. Kudo Y, Ogawa I, Kitajima S, Kitagawa M, Kawai H, Gaffney PM, et al. Periostin Promotes Invasion and Anchorage-Independent Growth in the Metastatic Process of Head and Neck Cancer. Cancer Res. 15 juill 2006;66(14):6928‑35.

28. Rachner TD, Göbel A, Hoffmann O, Erdmann K, Kasimir-Bauer S, Breining D, et al. High serum levels of periostin are associated with a poor survival in breast cancer. Breast Cancer Res Treat. avr 2020;180(2):515‑24.

29. Hu W, Jin P, Liu W. Periostin Contributes to Cisplatin Resistance in Human Non-Small Cell Lung Cancer A549 Cells via Activation of Stat3 and Akt and Upregulation of Survivin. Cell Physiol Biochem Int J Exp Cell Physiol Biochem Pharmacol. 2016;38(3):1199‑208.

30. Morra L, Rechsteiner M, Casagrande S, von Teichman A, Schraml P, Moch H, et al. Characterization of periostin isoform pattern in non-small cell lung cancer. Lung Cancer Amst Neth. mai 2012;76(2):183‑90.

31. Bonnet N, Biver E, Chevalley T, Rizzoli R, Garnero P, Ferrari SL. Serum Levels of a Cathepsin-K Generated Periostin Fragment Predict Incident Low-Trauma Fractures in Postmenopausal Women Independently of BMD and FRAX: PERIOSTIN FRAGMENT AND INCIDENT FRACTURE. J Bone Miner Res. nov 2017;32(11):2232‑8.

Figure 1: Overall survival according to median periostin value in the population of adenocarcinoma lung cancer patients (n=133; A) and restricted to the bone metastatic patients (n=66; B). Statistics: Log-rank test. NR: not reached.

Figure 2: Periostin immunostaining performed on bone metastases in patients with *KRAS*-mutated adenocarcinoma lung cancer. The antibody used was anti-total periostin-USCN®. Left column magnification x20. Dashed rectangle indicates the corresponding region of interest presented in the right column. ERxx corresponds to patient anonymization code. A strong stroma expression of periostin is present in ER13 and ER37 whereas it is absent or weak in ER34 and ER35. There is a nuclear and cytoplasmic expression of periostin in cancer cells in ER13, ER35 and ER52. Cancer cell periostin expression in ER34 is strong but heterogenous.

Figure 3: Periostin immunostaining performed on bone metastases in *Balb/c nude* mice injected with A549-*KRAS* cells. A) radiograph of bone metastasis at sacrifice (day 56). B) H&E staining (magnification X20). C and D) Immunostaining performed with antibody anti-periostin from USCN® on culture A549 cells showing no expression (C) and on bone metastasis sections showing tumor expression (D); magnification X20. E and F) Immunostaining performed with antibody anti-periostin from Biomedica® showing tumor expression (E: magnification X20; white band corresponds to 100µm. F: magnification X40; white band corresponds to 50µm). T: Tumor, BM: Bone matrix.

Supplemental figure 1: Comparaison of serum periostin (pmol/mL) in localized group vs paired controls (left) and in bone metastatic group vs paired controls (right). Statistics used: non parametric tests.

Supplemental figure 2: Periostin immunostaining performed on bone metastases in patients (n=5) with non-*KRAS* mutated adenocarcinoma lung cancers. ERxx corresponds to patient anonymization code. A-F: antibody anti-total periostin-USCN®. G and H) Negative control without primary antibody in mutated (ER52) and non-mutated (ER50) *KRAS* patient; magnification x20. E and F) Dashed rectangle indicates the corresponding region of interest presented in the right column. These sections also show heterogenous expression between patients. ER15, ER49 and ER50 had stroma reaction, ER43 had a weak expression, and ER45a cytoplasmic and nuclear expression.

Supplemental figure 3: Periostin immunostaining performed on bone metastases in patients with KRAS-mutated adenocarcinoma lung cancer. Antibody anti-total periostin-Biomedica®. There was a cytoplasmic and nuclear expression of periostin in tumor cells in the cases ER37 and ER13. By contrast, there is no tumor expression in case ER34. In case ER37, periostin was also expressed by periosteal tissue. These results are similar to that observed with the USCN® antibody. Magnification x20 (A) and x40 (B).

Table 1: clinical and laboratory parameters of the adenocarcinoma lung cancer population.

Table 2: Univariate and multivariate analysis of parameters associated with the risk of death

Table 3: Univariate and multivariate analysis of parameters associated with the risk of death in the bone metastatic group.

Figure 1

Click here to access/download;Figure;Figure 1_clean.pptx

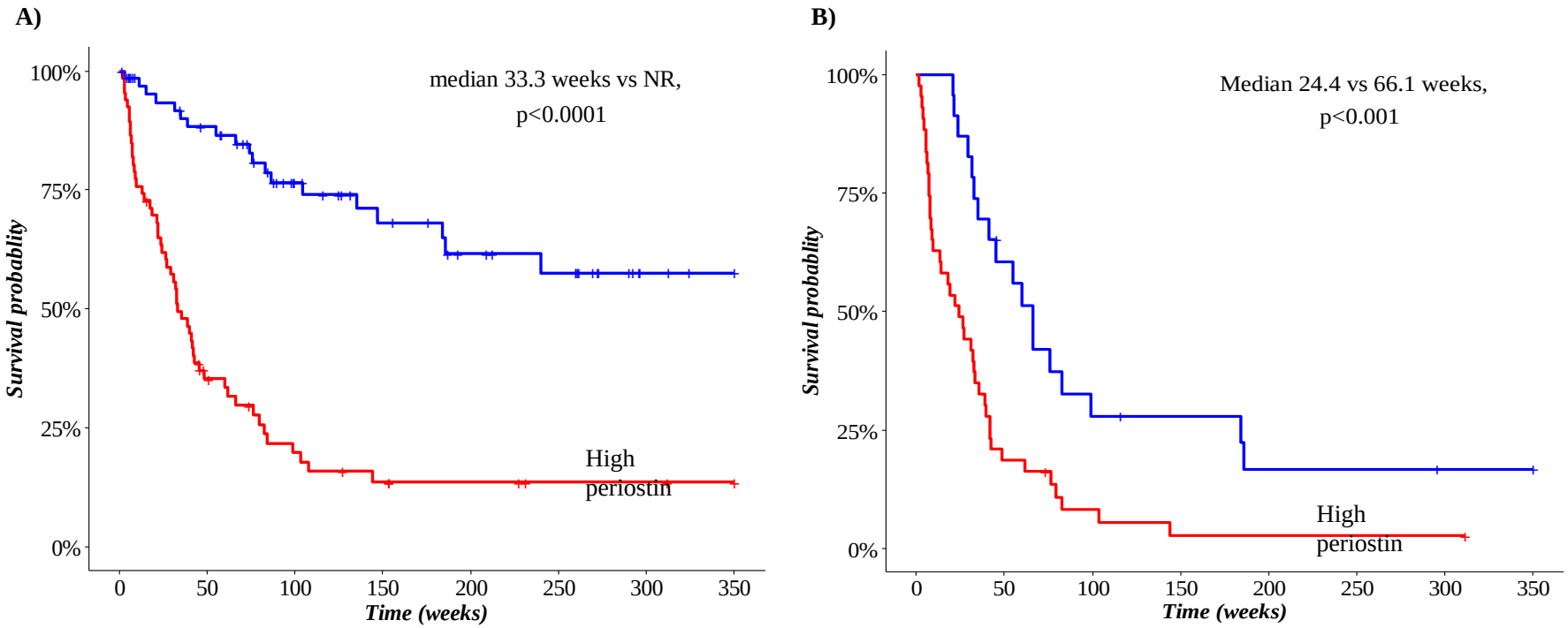


Figure 1: Overall survival according to median periostin value in the population of adenocarcinoma lung cancer patients (n=133; A) and restricted to the bone metastatic patients (n=66; B). Statistics: Log-rank test. NR: not reached.

Figure 2 revised

Click here to access/download;Figure;Revised_Figure 2_cleanJBO-EB.pptx

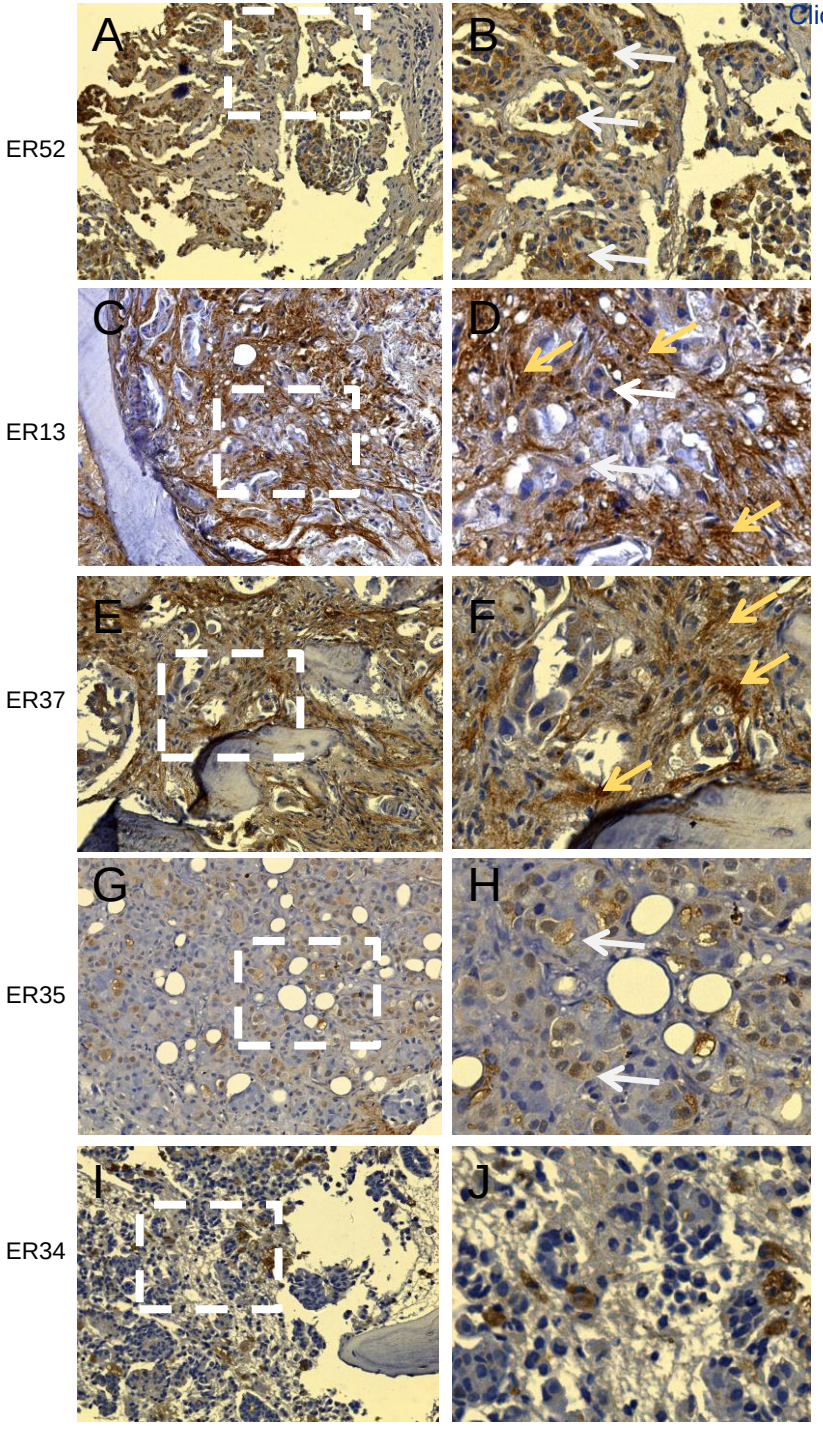


Figure 2: Periostin immunostaining performed on bone metastases in patients with *KRAS*-mutated adenocarcinoma lung cancer. The antibody used was anti-total periostin-USCN®. Left column magnification x20. Dashed rectangle indicates the corresponding region of interest presented in the right column. ERxx corresponds to patient anonymization code. A strong stroma expression (yellow arrow) of periostin is present in ER13 and ER37 whereas it is absent or weak in ER34 and ER35. There is a nuclear and cytoplasmic expression of periostin in cancer cells in ER13, ER35 and ER52 (white arrow). Cancer cell periostin expression in ER34 is strong but heterogenous.

Figure 3

Click here to access/download;Figure;Figure 3_clean.pptx

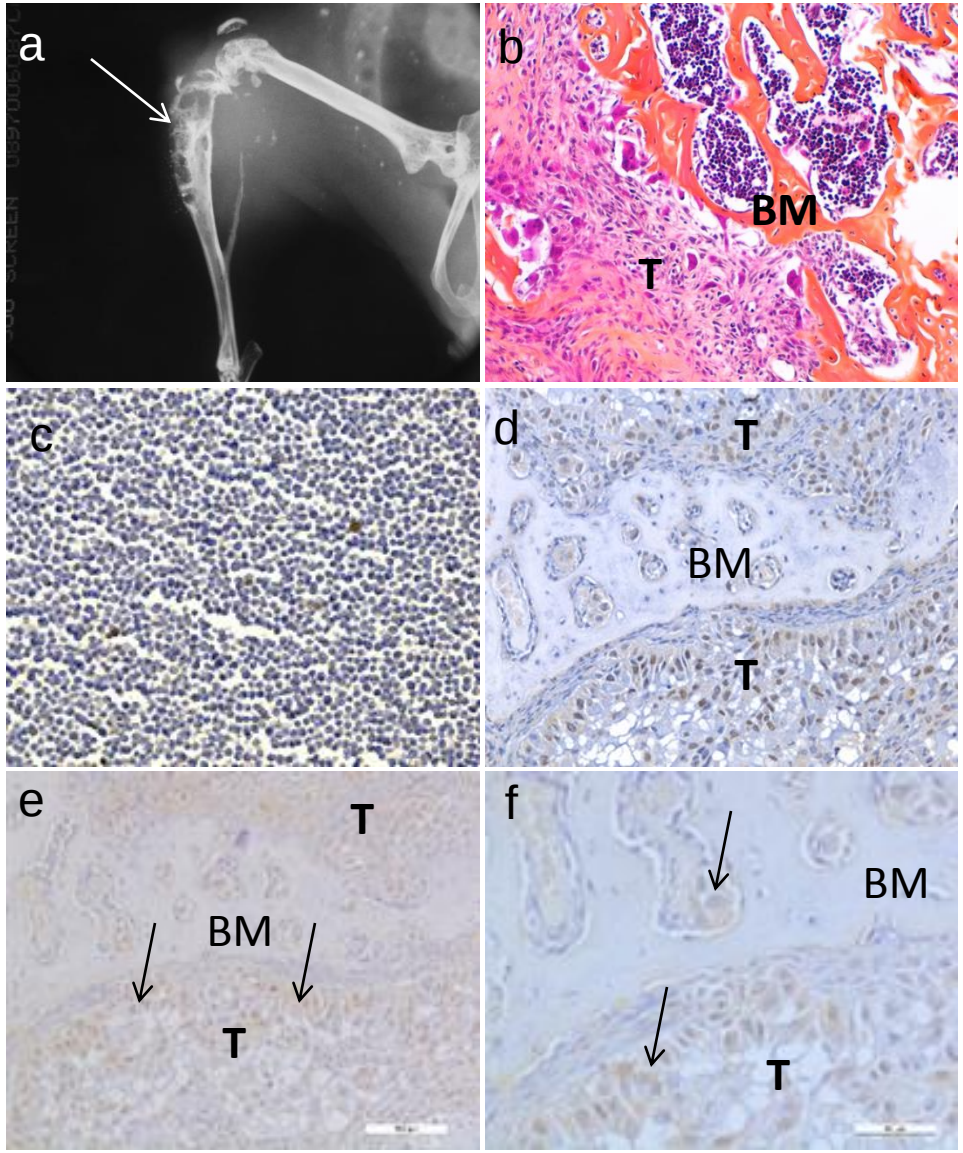


Figure 3 : Periostin immunostaining performed on bone metastases in Balb/c nude mice injected with A549-*KRAS* cells. A) radiograph of bone metastasis at sacrifice (day 56). B) H&E staining (magnification X20). C and D) Immunostaining performed with anti-periostin from USCN® on culture A549 cells showing no expression (C) and on bone metastasis sections showing tumoral expression (D) (magnification X20). E and F) Immunostaining performed with anti-periostin from Biomedica® showing tumoral expression (E: magnification X20; white band corresponds to 100µm. F: magnification X40; white band corresponds to 50µm). T: Tumour, BM: Bone matrix.

Click here to access/download;Table;Periostine_JBO_Table 1_revision_010421.docx

Table1: Clinical and laboratory parameters of the lung adenocarcinoma

Parameters		Whole population N=133	Bone metastatic patients N=66	Localized patients N=67	p value
Sex (male)		84 (63%)	48 (72%)	36 (53%)	0.03
Age (years)		63.5 ± 10.9	65.1 ± 11.6	61.8 ± 10.0	0.07
Adenocarcinoma		133 (100%)	66 (100%)	67 (100%)	-
Stage at diagnosis:	I	37 (28.5%)	0	37 (55.2%)	-
	II	17 (12.8%)	0	17 (25.4%)	-
	III	13 (9.8%)	0	13 (19.4%)	-
	IV	66 (48.9%)	66 (100%)		-
CRP (mg/L)		38.3 ± 60.8	59.9 ± 67.3	15.1 ± 42.4	0.00001
Neutrophils (G/L)		6.7 ± 6.2	7.4 ± 3.9	6.0 ± 7.8	0.22
Lymphocytes (G/L)		2.1 ± 1.7	1.9 ± 2.3	2.2 ± 0.8	0.37
Albuminemia (g/L)		35.9 ± 5.3	33.9 ± 5.6	37.8 ± 4.2	0.00002
Calcemia (mmol/L)		2.30 ± 0.1	2.30 ± 0.2	2.31 ± 0.1	0.24
BAP (µg/L)		32.5 ± 34	23.4 ±30.0	40.4 ± 35.7	0.002
CTXs (pg/l)		591.6 ± 347.8	700.0 ± 375.9	472.3 ± 256.8	0.00003
NLR		4.2 ± 5.1	5.1 ± 4.8	3.4 ± 5.4	0.06
ALI		278.2 ± 259.4	189.2 ± 161.3	344.3 ± 310.9	0.0005
Periostin (pmol/l)		1307 ± 655.9	1731.9 ± 681.5	888.8 ± 212.0	$8x10^{-15}$

Data are presented as mean ± standard deviation (SD) or n (%). CRP: C reactive protein
PNN: Neutrophil polynuclear cells. BAP: bone alkaline phosphatase. CTXs: serum carboxy-terminal collagen crosslinks. NLR: Neutrophil-Lymphocyte Ratio. ALI: Advanced Lung cancer inflammation Index. P value to test localized versus bone metastatic patients.

Click here to access/download;Table;Table 2.docx

Table 2: Univariate and multivariate analysis of parameters associated with the risk of death.

Univariate analysis : parameters	HR	95% CI	*p-value*
Age (one additional year)	1.02	0.99 - 1.05	0.05
Sex (male)	0.81	0.49 - 1.31	0.4
Metastatic group	7.51	4.60 - 12.3	<0.0001
High periostin	5.20	3.03 - 8.90	<0.00001
Periostin (per 100 pmol/l increase)	1.12	1.08 - 1.15	<0.0001
CRP (>10 mg/L)	2.79	1.78 - 4.38	0.0008
Neutrophils (>5.20 g/L)	1.86	1.19 - 2.91	0.006
Lymphocyte (<1.92 g/L)	1.77	1.13 - 2.79	0.01
Albuminémie (<37 g/L)	2.40	1.54 - 3.75	<0.0001
Calcemia (>2.52 mmol/L)	2.51	1.02 - 6.24	0.04
BAP (>15 UI/mL)	1.25	0.78 - 2.01	0.4
CTXs (>440 pg/ml)	1.53	0.96 - 2.47	0.07
NLR (>2.70)	2.61	1.65 - 4.13	<0.0004
ALI (<290.12)	3.96	2.27 - 6.90	<0.0001

Multivariate analysis : parameters	HR	95% CI	*p-value*
Periostin, high	2.09	1.06-4.13	0.03
Metastatic arm	2.80	1.59-4.95	0.0003
Age (one additional year)	1.01	0.99-1.05	0.25
CRP (>10 mg/L)	1.39	0.571-2.76	0.34
Calcemia (>2.52 mmol/L)	1.60	0.47-5.40	0.45
CTXs (> 440 pg/mL)	0.84	0.46-1.55	0.58
ALI (<290.12)	1.38	0.69-2.79	0.35

HR: Hazard ratio. CI: Interval confidence. High periostin refers to upper the median value of 1092 pmol/L.CRP: C reactive protein. CTXs: serum carboxy-terminal collagen crosslinks. NLR: Neutrophil-Lymphocyte Ratio. ALI: Advanced Lung cancer inflammation Index.

Click here to access/download;Table;Table 3.docx

Table 3: Univariate and multivariate analysis of parameters associated with the risk of death in the bone metastatic group.

Univariate analysis : parameters	HR	95% CI	p-value
Age	1.01	0.99 - 1.04	0.4
Sex (male)	0.92	0.51 - 1.65	0.8
High periostin	2.59	1.47 - 4.58	0.001**
Periostin (per 100 pmol/l increase)	1.05	1.02 - 1.09	0.004**
CRP (>10 mg/L)	0.68	0.39 - 1.20	0.2
PNN (>5.20 g/L)	1.55	0.89 - 2.69	0.1
Lymphocyte (<1.92 g/L)	0.78	0.44 - 1.39	0.4
Albuminemia (<37 g/L)	0.50	0.27 - 0.91	0.02*
Calcemia (>2.52 mmol/L)	0.22	0.03 - 1.63	0.1
BAP (>15 µg/L)	0.87	0.48 - 1.57	0.6
CTXs (>440 pg/ml)	0.76	0.39 - 1.35	0.3
NLR (>2.70)	1.39	0.79 - 2.45	0.2
ALI (<290.12)	1.60	0.84 - 3.87	0.2

Multivariate analysis : parameters	HR	IC 95%	p-value
High periostin	3.62	1.74 - 7.52	0.0005***
Age (one additional year)	1.00	0.97 - 1.03	0.77
CRP (>10 mg/L)	0.99	0.46 - 2.10	0.97
Calcemia (>2.52 mmol/L)	0.13	0.01 - 1.01	0.05
CTX (>440 pg/ml)	0.67	0.32 - 1.39	0.28
ALI (<290.12)	1.47	0.65 - 3.28	0.34

HR: Hazard ratio. IC: Interval confidence. High periostin refers to upper the median value of 1752 pmol/L.CRP: C reactive protein. CTXs: serum carboxy-terminal collagen crosslinks. NLR: Neutrophil-Lymphocyte Ratio. ALI: Advanced Lung cancer inflammation Index.

Supplemental figure 1

Click here to access/download
Supplementary Material
SupplFig1_POumosPosn_v21oct2020_uniteAjourLeftRight.pptx

Supplemental figure 2



Click here to access/download
Supplementary Material
+SupplFig2_Poumos_Posn_v21oct2020_legendeResized Clean.pptx

Supplemental figure 3



Click here to access/download

Supplementary Material

+SupplFig3_Poumos_Posn_v21oct2020_clean.pptx

Supplementary Figure 4



Click here to access/download

Supplementary Material

SupplementalFig4_IHC_POSTN_CT_20x.tif